Available online at www.sciencedirect.com
SCIENCE DIRECT®
International Journal of Machine Tools & Manufacture 45 (2005) 1504–1514
INTERNATIONAL JOURNAL OF MACHINE TOOLS & MANUFACTURE DESIGN, RESEARCH AND APPLICATION
www.elsevier.com/locate/ijmactool

Loading path optimization of tube hydroforming process

M. Imaninejad, G. Subhash*, A. Loukus

Department of Mechanical Engineering-Engineering Mechanics, Michigan Technological University, Houghton, MI 49931, USA

Received 4 August 2004; accepted 20 January 2005
Available online 7 March 2005

Abstract

Optimization methods along with finite element simulations were utilized to determine the optimum loading paths for closed-die and T-joint tube hydroforming processes. The objective was to produce a part with minimum thickness variation while keeping the maximum effective stress below the material ultimate stress during the forming process. In the closed-die hydroforming, the intent was also to conform the tube to the die shape whereas in the T-joint design, maximum T-branch height was sought. It is shown that utilization of optimized loading paths yields a better conformance of the part to the die shape or leads to a higher bulge height. Finite element simulations also revealed that, in an optimized loading path, the majority of the axial feed needs to be provided after the tube material yields under the applied internal pressure. These results were validated by conducting experiments on aluminum tubes where a good correlation between the experimental results and simulations were obtained.

Keywords: Tube hydroforming; Optimization; Finite element analysis; Aluminum alloys

1. Introduction

Rapid growth of computational facilities in the last few decades has assisted researchers to invoke numerical and analytical methods in analysis and design of diverse mechanical problems. Central to these enhancements are finite element (FE) software packages that have emerged as an essential tool in design and analysis. Although most FE software would carry out the computational portion of the problems, the importance of user interaction in suitably incorporating the boundary conditions, material properties, loading trajectories, etc, cannot be disregarded. Based upon the problem definition, various experiments or analyses may be required to determine the necessary parameters.

Manufacturers and designers always strive to develop loading trajectories that would result in the optimized characteristics of the final product. For instance, low residual stresses, good surface finish and uniform thickness distribution are desirable for most manufactured parts. Although these factors are affected by the material used, they are also a function of forming process parameters and loading conditions.

In most forming processes the attainable strains are path-dependent [1]. Thus, the formability characteristics of a product are a function of the loading trajectory during forming operation. Since the stress induced in a material is a function of the strain path, in processes such as tube hydroforming where multiple loads are applied, the sequence and magnitude of each load would influence the final characteristics of the product. Therefore, it would be of interest to form the material in a manner that results in the desired characteristics in the final part, i.e. maximize the minimum part thickness, minimize the residual stresses, attain the maximum formability, etc. In the past, manufacturers used to construct 'try-outs' and employ trial and error methods to optimize the loading paths. In many cases these methods would not yield a cost-effective solution and could be time-consuming. Incorporating optimization methods along with 'design of experiments' methods and 'finite element' simulations have been proven to be a powerful tool to overcome many of the above problems.

In recent years, researchers have focused on optimization of loading trajectories for different tube hydroforming processes [2–6]. Yang et al. [4] developed a FE code combined with an optimization tool to determine

* Corresponding author. Tel.: +1 906 487 3161; fax: +1 906 487 2822.
E-mail address: subhash@mtu.edu (G. Subhash).

0890-6955/$ - see front matter © 2005 Elsevier Ltd. All rights reserved.
doi:10.1016/j.ijmachtools.2005.01.029

Nomenclature

p	design variable	K	strength coefficient
$f(p)$	cost function	n	strain hardening coefficient
$g(p)$	constraint function	P	pressure
D	feasible domain	S	single-stroke end feed
t_o	initial thickness	D	double-stroke end feed
t_i	final thickness	Q	quadruple-stroke end feed
$\bar{\sigma}$	effective stress	V	bulge control distance
σ_u	ultimate tensile stress		

the optimum loading paths for tube hydroforming processes. Their results showed a substantial enhancement in thickness reduction for a closed-die and a sub-frame. Fann and Hsiao [5] developed an optimization approach based on conjugate gradient method utilizing FE simulations. The above code was utilized to optimize the loading trajectory of a T-shape process based on batch mode and sequential mode. They concluded that sequential mode generated a loading path that is less prone to geometrical errors compared to other methods. Aue-U-Lan et al. [6] evaluated different optimization approaches and conducted FE simulations and experiments of a closed-die tube hydroforming. Their simulation showed a good correlation with experiments.

In this paper, finite element simulation (using LS-DYNA) and optimization software (LS-OPT) are used to optimize the loading paths for closed-die and T-branch tube hydroforming experiments. The intent of the optimization procedure is to determine the loading paths that would result in a product with a uniform thickness distribution, maximum effective stress less than the ultimate stress and realize the maximum attainable formability of the material.

2. Loading path optimization

Recalling an optimal design problem that can be generally represented as [4]

$$\begin{aligned} &\text{optimize } f(p), && p \in D \\ &\text{subject to } g_i(p) \le 0, && i = 1, 2, \ldots m \end{aligned} \tag{1}$$

where $f(p)$ is the 'objective' or 'cost' function that needs to be minimized, p is design variable, D is feasible domain and $g_i(p)$ are the 'constraint' functions.

From design and manufacturing point of view, a well-qualified hydroformed part must meet the following conditions: (i) conform to the die shape (or reach the maximum attainable formability) (ii) have a uniform thickness distribution and (iii) not experience any failure while being formed.

Since some die geometries may not have a closed cavity, e.g. T-joint, Y-Shape, etc. the condition (i) needs to be defined based on the geometrical features of the problem. Researchers have defined the second condition in various fashions. Fann and Hsiao [5] defined the difference between the maximum and minimum thickness as the 'objective' function. However, if thickness uniformity along the tube is desired one can define the 'objective' function as

$$f(p) = \sqrt{\sum_{i=1}^{N} \left(\frac{t_i - t_o}{t_o} \right)^2} \tag{2}$$

where $f(p)$ is the thickness deviation, t_i and t_o represent the final thickness and initial thickness of the element i, respectively, and N represents the total number of elements.

In most cases, conditions (i) and (ii) denote the 'constraints' of the problem. However, in cases such as T-joint process where there is no die-induced limit on the branch height (a higher T-section is often desirable), the first condition can play the role of another objective function. In other words, the actuator perpendicular to the tube axis in the T-section (bulge controller) can be controlled to move further away from the tube axis to create a higher T-branch. Although the above prescribed objectives and constraints were identified based on the utilized hydroforming schemes, it should be emphasized that these may vary with regard to the desired characteristics of the final product, geometrical features and problem definition. Among other parameters or functions that may be implemented as objectives or constraints in hydroforming applications are minimum thickness of the tube, forming limits, failure criterion, conformance of the tube to some specified geometrical features of the die, etc.

The above optimization procedure is employed (using LS-DYNA and LS-OPT) in the following to optimize the loading paths (i.e. axial feed, internal pressure and bulge controller if applicable) of a closed-die and T-joint hydroforming experiments. A constant pressurizing rate is considered and the maximum internal pressure is determined. To feed the material into the forming zone, single and multiple linear axial feeds are employed and displacement of the tube-ends after each stroke is established. Both simulations are designed to achieve a uniform thickness distribution below a certain stress limit. However, the objective of the closed-die simulation is also

to have the tube to conform to the shape of the die whereas in the T-joint modeling, a higher T-branch is desired.

2.1. Closed-die

Closed-die tube hydroforming is the most common process in tube hydroforming industry. In this method, after the tube is placed in the die, it is pressurized while its ends are being pushed axially into the die to conform to the die shape, see Fig. 1(a). Die shapes may vary from simple symmetrical to complicated shapes with uncommon geometries. Researchers have conducted numerous studies to explore different numerical and experimental issues of this process [2,7,8].

2.1.1. Loading path optimization of closed-die

To conduct closed-die tube hydroforming experiments on AA6063 in the T4 condition (solution treated, quenched, and naturally aged), a symmetric closed-die was designed, as shown schematically in Fig. 1(a). The goal of this study was to determine the optimized internal pressure and axial feed trajectory that would result in complete conformance of the tube to the die and also yield a uniform thickness distribution along the hydroformed section. Hence, the optimization problem can be outlined as

Objective (1): **Minimize** thickness deviation (Eq. (2))

Objective (2): **Minimize** ($\text{Volume}_{\text{Die}} - \text{Volume}_{\text{Tube}}$)

Constraint (1): $\bar{\sigma}_i < \sigma_u$

Where $\bar{\sigma}_i$ and σ_u represent the effective stress field and the material ultimate tensile stress, respectively. Objective (1) aims for a uniform thickness distribution, whereas objective (2) intends to conform the tube to the die shape. Although objective (2) could be defined as a constraint (instead of objective), since there was no assurance of the full conformance of the tube to the die without failure, it was defined as an objective. Hence, the intent is to either have the tube to conform to the die shape (such as closed-die) or reach the maximum attainable formability. Based on the above discussion, the ideal situation would be ($\text{Volume}_{\text{Die}} - \text{Volume}_{\text{Tube}}$) = 0, where the outer surface of the tube is fully conformed to the inner shape of the die. Constraint (1) also describes the feasible domain for the effective stress. In other words, since the maximum stress that the material can carry is equal to the ultimate stress, the maximum effective stress in the tube material should not exceed σ_u throughout the process.

Using shell elements, a tube of 200 mm length, 38.1 mm diameter and 3.18 mm thickness was modeled in HyperMesh v5 (see Fig. 1(b)). Earlier studies by the authors [9,10] revealed that using material parameters (in power-law model) obtained from simple tensile tests of curved specimen [ASTM-B557M] would yield a better estimation of the bulge height vs. internal pressure during free-end and pinched-end hydroforming of aluminum extrusions compared to flat tensile specimen [ASTM-B557] data. Tensile test data on the curved

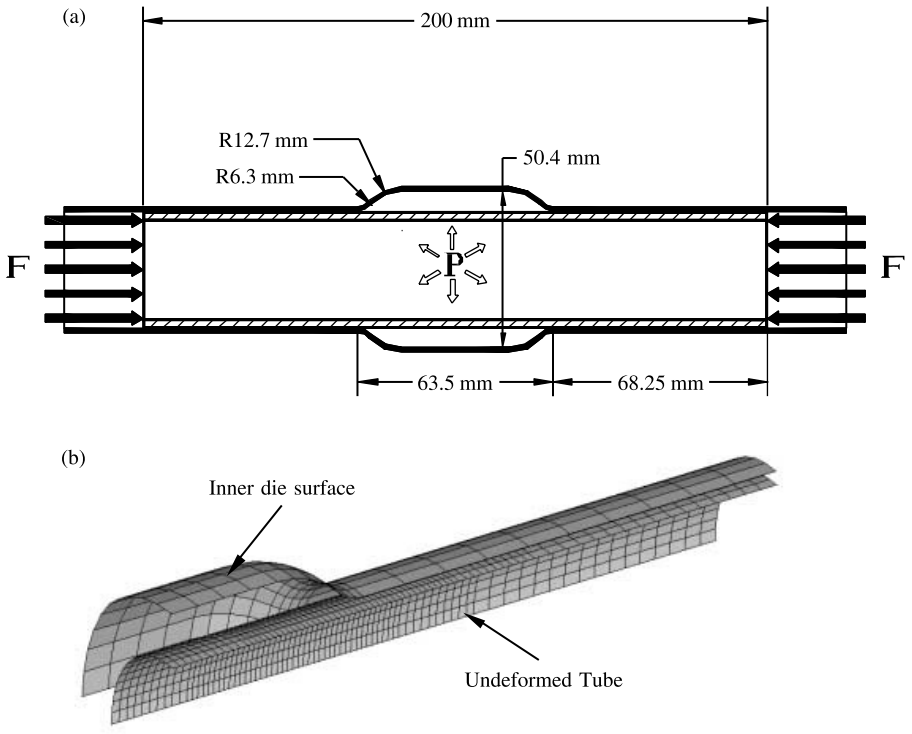

Fig. 1. (a) Schematic of the closed-die and (b) undeformed finite element model of 1/8th of the tube and the closed-die.

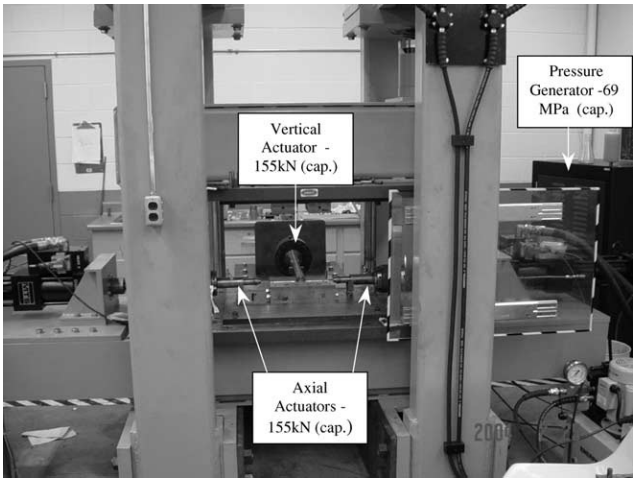

Fig. 2. Hydroforming press at Michigan Technological University capable of 68 MPa of internal pressure and 3600 kN closing force.

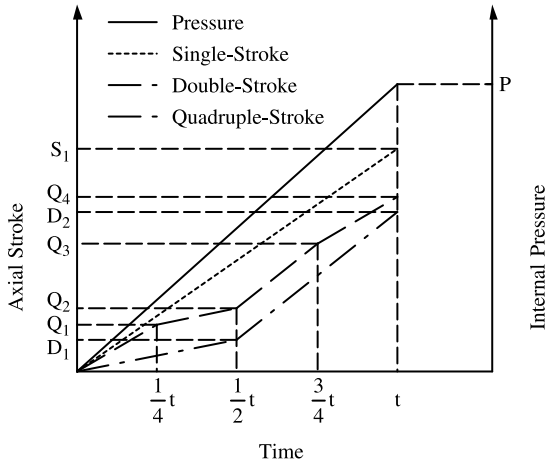

Fig. 3. Schematic of pressurizing and axial feed paths for closed-die hydroforming.

specimen (cut from tube cross section) were curve fit to the power law model ($\bar{\sigma} = K\bar{\varepsilon}^n$) and yielded a K-value of 265.2 MPa and n-value of 0.166 [9]. A coulomb friction coefficient of 0.05 was utilized at all contact areas [9]. The hydroforming equipment utilized in these experiments is also shown in Fig. 2. The equipment consists of two 155 kN actuators to feed the material in the axial direction and a vertical actuator that controls the branch height of the T-branch configuration. Because axial actuators used in the experiments were displacement-controlled, 'prescribed motion' was assigned to the tube-ends to simulate the end-movement of the tube into the die region. The pressure intensifier used in this experiment was capable of providing only one linear pressurizing rate throughout the test. However, the axial feed could be applied in a non-linear fashion, if desired.

To assess the influence of these two independent parameters, two types of simulations were performed. In the first set of simulations, the maximum internal pressure was limited to the range of 40–50 MPa. This will be referred to as 'lower pressure' simulations. In the second set, referred to as 'high pressure' simulations, the maximum internal pressure range was prescribed between 50 and 80 MPa. The motivation for these two sets of simulations is to delineate the effect of low pressure (where the axial feed is expected to play a dominant role in the forming process) and high pressure (where the internal pressure may have a more significant role and the axial feed may provide just the sufficient amount of material flow into the forming region) on the resulting tube geometry.

To describe the axial displacement movement of the tube-ends single-stroke (S), double-stroke (D) and quadruple-stroke (Q) functions (see Fig. 3) consisting of one, two and four linear end-movements were employed, respectively. The ultimate stress obtained during the tensile tests ($\sigma_u = 210$ MPa) was defined as the maximum tolerable von Mises stress in the tube material (constraint). Since the tube hydroforming processes were to be performed at room temperature, the material was not considered rate-sensitive and the total computational time was reduced to 0.05 s. LS-OPT v2a was utilized to conduct the optimization process. End movement (S, D or Q) and internal pressure (P) were employed as design variables, see Fig. 3. Due to the limited capability of the pressure intensifier available, only one linear pressurizing rate could be assigned to the process. Hence, the only unknown in the simulation was the final pressure (or the pressurizing rate). However, the rate of end-displacement could vary at different points throughout the process. In the first set of simulations, it was considered that the end-feed rate is constant throughout the process, i.e. single-stroke. In double-stroke experiment, the end-feed rate could change at some intermediate stage during the experiment. Therefore, the final end-feed (D_2) and the end-displacement at the intermediate stage (D_1) were to be optimized, see Fig. 3. In the last set of simulations, four different end-feed rates were considered at equal time intervals during the simulation, i.e. quadruple-stroke (Q_1, Q_2, Q_3 and Q_4). This gives the opportunity to achieve more complex loading trajectories.

Table 1 summarizes the single-, double-, and quadruple-stroke optimized axial feeds and the maximum internal pressures derived for the low pressure and high pressure simulations. This table reveals that utilizing higher final internal pressure in each case yields a slightly larger thickness variation (Eq. (2)) compared to the lower pressure situations. This is due to the severe thinning of the tube in the bulged area. Recall that in higher pressure simulations, the axial feed occurs at much later stage and the tube expands due to the dominance of hoop stress, thus resulting in rapid thinning. Although hydroforming with a higher maximum internal pressure seems to yield a better conformance of the tube to the die (i.e. minimum volume

Table 1
Optimized pressures and strokes for closed-die hydroforming

	Single-stroke		Double-stroke		Quadruple-stroke	
	Low pressure	High pressure	Low pressure	High pressure	Low pressure	High pressure
Pressure (MPa)	50.00	62.09	46.82	61.99	47.33	76.48
Stroke (mm)	$S_1=9.79$	$S_1=6.3$	$D_1=3.54$	$D_1=3.22$	$Q_1=0.95$	$Q_1=0.96$
			$D_2=10.17$	$D_2=5.74$	$Q_2=2.97$	$Q_2=5.10$
					$Q_3=5.95$	$Q_3=5.10$
					$Q_4=9.49$	$Q_4=6.59$
Thickness deviation (Eq. (2))	13.17	13.64	13.17	13.71	13.23	13.58
$(V_{Die}-V_{Tube})/V_{Die}$	0.109	0.106	0.103	0.08	0.082	0.078

deviation between die and tube, see the last row), severe thinning at the center of the expansion zone may lead to premature failure of the tube. It is also seen that in all the optimization schemes employed, a higher axial feed (stroke) is required to conform the tube to the die shape whenever a lower pressure is utilized. This implies that when lower pressures are used, the axial feed plays a more significant role in assisting the material to flow into the forming zone compared to the higher pressures experiments. However, it should be noted that in higher pressure situations, the internal pressure tends to be the dominant force that causes the material to expand and conform to the die shape. Table 1 also reveals that in both low and high pressure simulations, utilization of multiple-strokes yields better conformance of the tube to the die. Further investigation of the stress distribution along the tube also revealed that the majority of axial feed should be provided after the material yields plastically. As one can recall, when a material is in its plastic state, small stress increments result in a large increase of strain. However, this may also result in thinning and subsequent failure. Therefore, to achieve a uniform thickness distribution and prevent potential thinning, additional material needs to be fed into the forming region by providing sufficient axial feed when the plastic flow initiates. This validates the results that the majority of the axial feed must be provided during the final stages of hydroforming after the material yields due to the applied lower pressure. On the contrary, when higher internal pressure is utilized, tube material yields earlier and hence the maximum end-feed should be provided during the early stages of the process.

Fig. 4 depicts the thickness variation along the tube length for single-, double-, and quadruple-stroke cases. For all these simulations, thickening occurs at the tube-ends (where the axial force is applied) due to the concentrated load at this region. These figures also reveal that applying lower internal pressure results in higher material thickening at the die entry. This is because of the large axial feed, lack of sufficient internal pressure which can force the material into the expansion zone, and finally, the change in the direction of material flow at this location. Employing higher pressure also results in a more uniform thickness change in the expansion zone. But the severity of thinning is significantly greater and may lead to failure as will be discussed later in hydroforming experiments. However, since no failure criterion was incorporated in the simulations, failure location could not be predicted. As will be illustrated in Section 2.1.2, both higher pressure and lower pressure experiments showed different thickness distributions along the tube. In both simulations, the number of strokes did not have a significant influence on the tube final thickness.

2.1.2. Experimental results of closed-die tube hydroforming

To validate the above optimization simulation results, closed-die experiments were performed on extruded AA6063-T4 tubes of 38.1 mm outer diameter, 3.18 mm wall thickness, and 200 mm length. These tubes were supplied by Hydro Aluminum Technology Center NA, Holland, Michigan. Tube hydroforming experiments were conducted in the aforementioned closed-die (Fig. 1(a)) using the hydroforming equipment at Michigan Technological University [9]. EcoForm HFL 5936-AG was used as a lubricant on the inside surface of the die cavity before each test.

After the tube was placed in the die cavity, plungers were brought into contact with the tube-ends applying a small axial force. This force is required to seal the tube-ends while filling the tube with fluid in the early stages of the experiment. During this stage air bubbles that may have been trapped in the tube were evacuated. After the die closure, axial feed and internal pressure were applied simultaneously with an intent to conform the tube to the shape of the die. Single-, double-, and quadruple-stroke functions as determined by the optimization simulations (Table 1) were employed. For each experiment, internal pressure was linearly ramped to the final optimized values. Fig. 5 shows the samples of hydroformed tubes with various optimized strokes. As one can see, when lower pressure loading paths were utilized all the tubes were able to fully conform to the shape of the die without failure, see Fig. 5(a). However, during the higher pressure experiments, all the tubes burst at the center of the bulging zone and were unable to conform to the die shape as seen in Fig. 5(b). Recalling

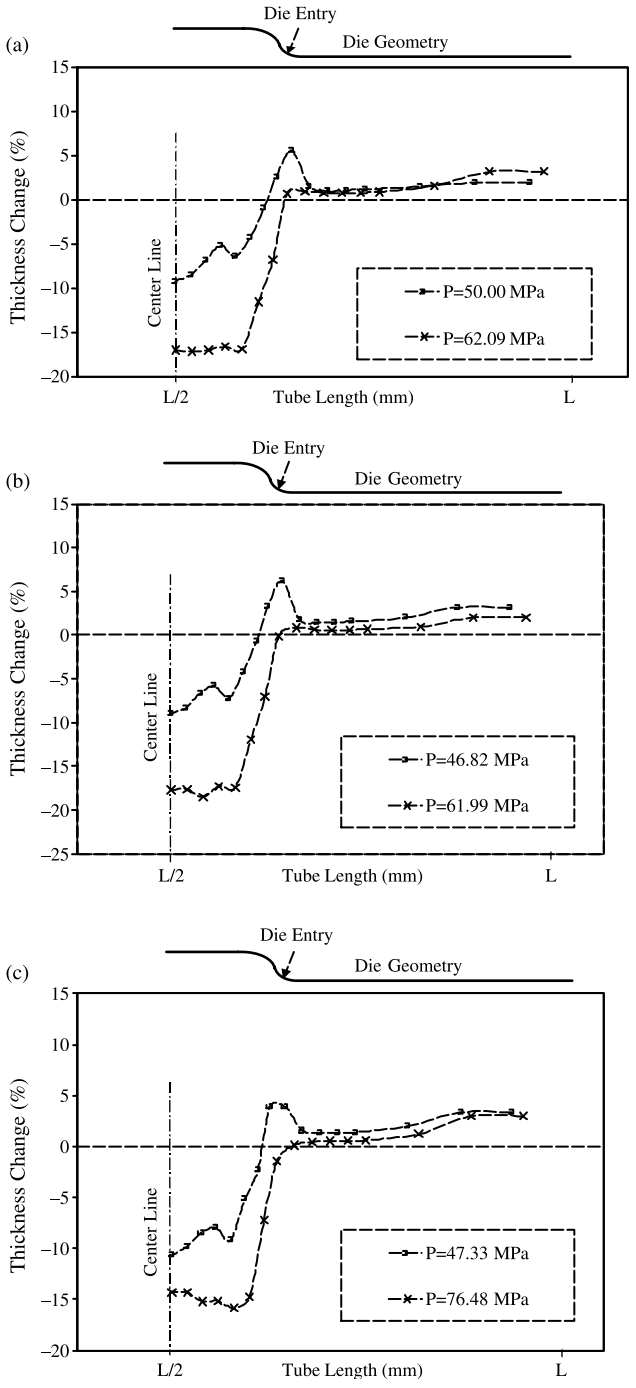

Fig. 4. Thickness distribution along the tube length for different pressures during closed-die tube hydroforming for (a) single-stroke, (b) double-stroke and (c) quadruple-stroke. For convenience of visualization the die geometry is also indicated.

the discussions in the FE from the preceding section, in all the higher pressure experiments, maximum thinning tends to occur in the expansion region Also, note from Table 1 that in these higher pressure simulations the axial feed is significantly smaller than that for lower pressure simulations. Therefore, in the absence of sufficient material flow into the forming zone at appropriate time, the material failure is bound to occur. Table 2 summarizes the maximum bulge height and hoop strain measurements of the hydroformed tubes employing higher pressure loading paths after the burst. It is clear that a higher bulge heights and hoop strains were achieved when quadruple-stroke is utilized. In other words, when material is fed into the forming zone in an optimized manner with multiple strokes, severe thinning and failure may be delayed and a higher bulge height can be obtained. Nevertheless, since no failure criterion was incorporated in simulations (for computational efficiency) they were unable to predict the burst and the tube did not conform to the die shape.

To further validate the simulation results, the fully conformed tubes shown in Fig. 5(a) were sectioned and the thickness of the tubes was measured along the length. Fig. 6 shows the thickness change along the length of the hydroformed tube for lower pressure single-stroke optimized path. For comparison purposes FE results are also shown. Evidently, the experimental results are in good agreement with the trends in the FE simulation. Since the FE results shown earlier in Fig. 4 revealed that the thickness distribution follows the same trend for all the low pressure experiments regardless of the number of strokes, result for only one experiment, i.e. single-stroke is compared to the experimental observations in Fig. 6.

Clearly, the optimization procedure employed above seems to provide reasonable estimation of internal pressure and axial feed paths that results in good conformation of the tube to the desired die features. The observed trends in the experimental measurements (Fig. 6) also correlate well with the simulations. Therefore, the above optimization method was employed to embark on the next level of complexity in hydroforming by attempting to optimize the loading trajectory of a T-joint die as will be discussed in the next sections.

2.2. T-joint Die

T-joints may be the first hydroformed parts that were commercially used in (sanitary) industry. To date, T-joints are utilized in many products such as engine cradles, frames, camshaft, etc, and are increasingly more popular due to their unique advantages such as fewer secondary operations, more stiffness, etc. Many researchers have investigated different aspects of the process analytically and experimentally [5,11,12–15]. Mac Donald and Hashmi [11] carried out a systematic FE study to investigate the effects of internal pressure, combination of internal pressure and axial load, friction and tube wall thickness, etc. on forming of a cross-joint. They concluded that employing internal pressure without applying axial feed would result in severe thinning in the branch top. Whereas, invoking axial feed in the simulation will increase the cross-branch height and would lessen the thinning in the branch top. They also obtained a good correlation with experimental results of tube thickness

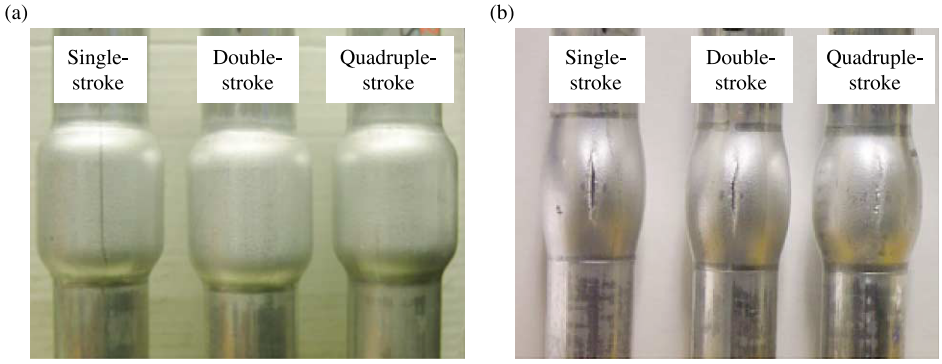

Fig. 5. Samples of closed-die hydroformed tubes employing optimized (a) lower pressure optimized loading paths and (b) higher pressure loading paths.

at several locations. Ahmed and Hashmi [12] presented their FE simulation on bulge forming of T-branches. Keeping a constant rate of axial feed, they performed simulations with different pressurizing rates. It was noticed that in the case with lesser pressurizing rate, lower effective stress and more uniform strain distributions were achieved compared to the higher pressurizing rate. More recently, Fann and Hsiao [5] investigated the optimization of the loading path for a T-joint part, but the use of a third actuator was not reported in their study.

Many other methods have been also used in the formation of a T-branch. Marreco and Al-Qureshi [13] established a novel method using elastomer rods inside metal tubes as the forming media. Later, Al-Qureshi and Moriera Filho [14] reported their work on junction formation of aluminum tubes using elastomer method. Al-Qureshi and Moriera Filho [15] also developed elastomer forming machine capable of forming various shapes. They have shown that this method could be a simple and could provide cost effective solution to some commercial forming applications. Elastomer forming for more complex shapes such as cross-junction can be found in the work by Filho and Al-Qureshi [15]. Although these methods can precisely produce components with the desired final shape, hydroforming of T-joints appears to be a more viable and faster manufacturing method.

Table 2
Maximum bulge height obtained from tube hydroforming experiments utilizing higher pressure loading paths

	Intended internal pressure (MPa)	Utilized internal pressure (MPa)	Maximum bulge height (mm)	Maximum hoop strain (True)
Single-stroke	62.09	35.67	4.55	0.214
Double-stroke	61.99	36.28	4.85	0.227
Quadruple-stroke	76.48	34.87	5.7	0.262

2.2.1. Loading path optimization of T-joint

In most hydroformed T-joints, although the tip of the branch may be cut and trimmed for manufacturing purposes, a uniform thickness distribution along the T-branch walls and bigger branch heights are often desirable. Hence, the optimization problem can be defined as

Objective (1): Minimize thickness deviation (Eq. (2))

Objective (2): Maximize branch height

Constraint (1): $\bar{\sigma}_i < \sigma_u$

Fig. 7(a) shows the schematic of a T-joint die, which was modeled using HyperMesh v5 and exported to LS-DYNA v960, see Fig. 7(b). It should be emphasized that use of vertical actuator '**V**' assists in controlling the material flow in the forming zone and in obtaining a higher bulge height with a flat top. A tube made of AA6063-T4 with the dimensions described earlier (for closed-die) was modeled using quadratic shell elements. Die geometry was modeled using rigid shell elements. A linearly increasing function was assigned to the internal pressure, similar to the previous experiments. Optimization simulations were performed using single-, double-, and quadruple-stroke displacement functions for

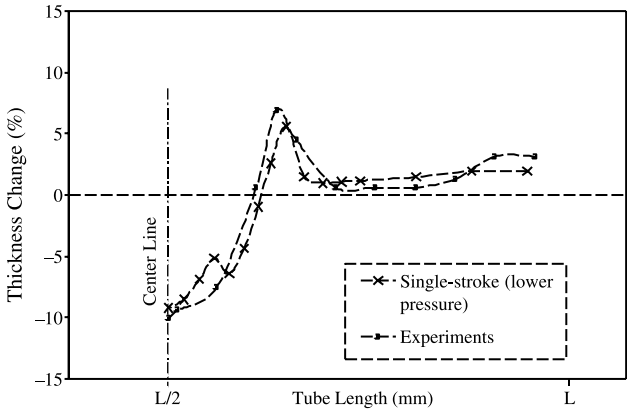

Fig. 6. Comparison between FE simulations and measured thickness distribution from the experiments along the tube length (single-stroke).

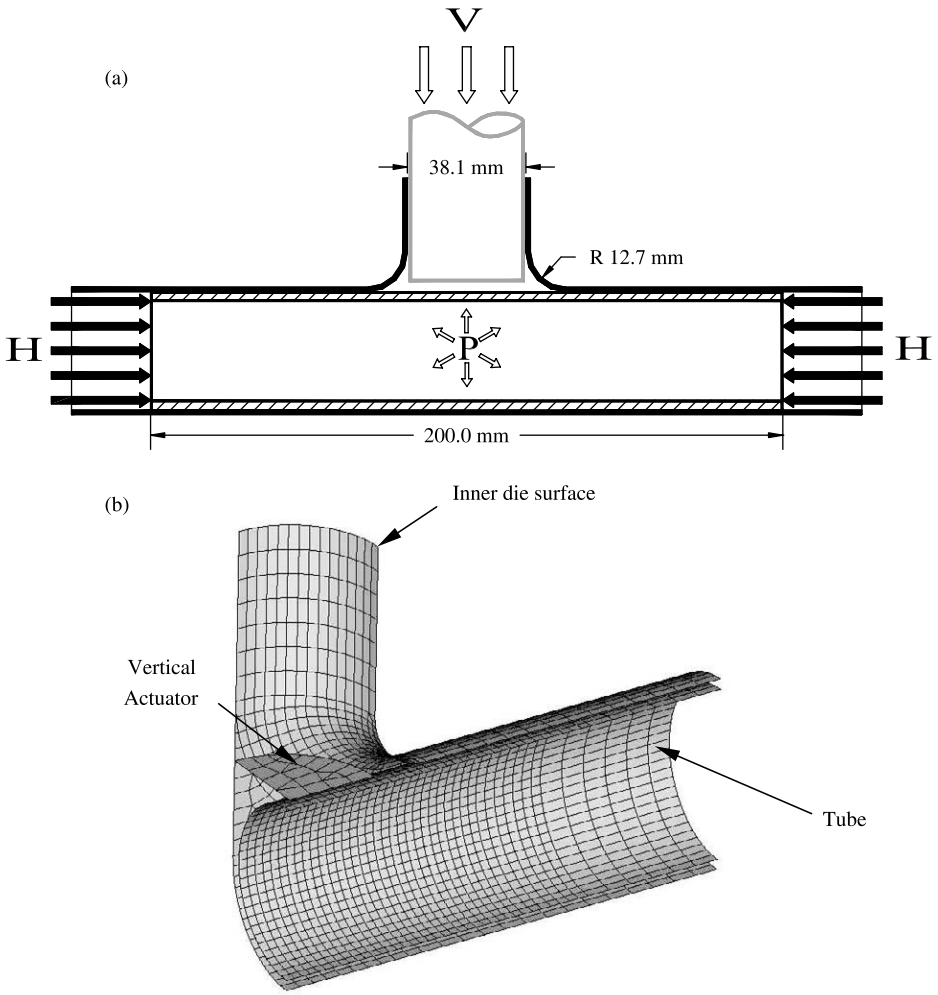

Fig. 7. (a) Schematic of the T-joint die and (b) undeformed finite element model of 1/4th of the tube and T-joint die.

the horizontal and perpendicular actuators. Fig. 8 illustrates the pressurizing path and the stroke functions to describe the displacement of the horizontal and the perpendicular actuators. Based on the objectives and constraint defined above, three design variables, i.e. internal pressure (P), axial displacement of the horizontal actuators (H) and axial displacement of the vertical actuator (V) at different time steps were required to be determined. The optimization study was performed using LS-OPT. Since a linear pressurizing rate was assigned to the internal pressure, the only unknown to be determined (with regard to pressure) was the maximum internal pressure. In the first set of the optimization simulations, a linear end-feed rate was assigned to both the axial and the vertical actuators. In other words, these actuators were made to move with a constant rate throughout the simulation (single-stroke). Whereas in the double-stroke and quadruple-stoke simulations, the axial feed (H) and bulge control (V) rates were allowed to change once and three times, respectively, during the simulation.

Table 3 shows the maximum internal pressure (P), axial feed (H) and control bulge (V) for optimized single-stroke, double-stroke and quadruple-stroke simulations. This table reveals that there is not a significant change in the maximum internal pressure when either the single- or the double- or the quadruple-strokes are employed. However, utilizing multiple strokes increases the bulge height as well as the maximum hoop strain significantly. This behavior has also been shown in the literature in elastomer forming [13,14]. Additional investigation of stress distribution in the T-section of these different paths suggested that to obtain a uniform thickness distribution along the tube, major axial feed needs to be provided after the material in the forming zone yields (plastic flow starts). This also supports the same conclusion gained from the closed-die simulations. Fig. 9 demonstrates the thickness variation along the tube for single-, double-, and quadruple-stroke cases. It is seen that in all situations thickening occurs at the tube-ends (where the axial feed is applied to push the tube into the die) and the maximum thickening at the die entry probably due to

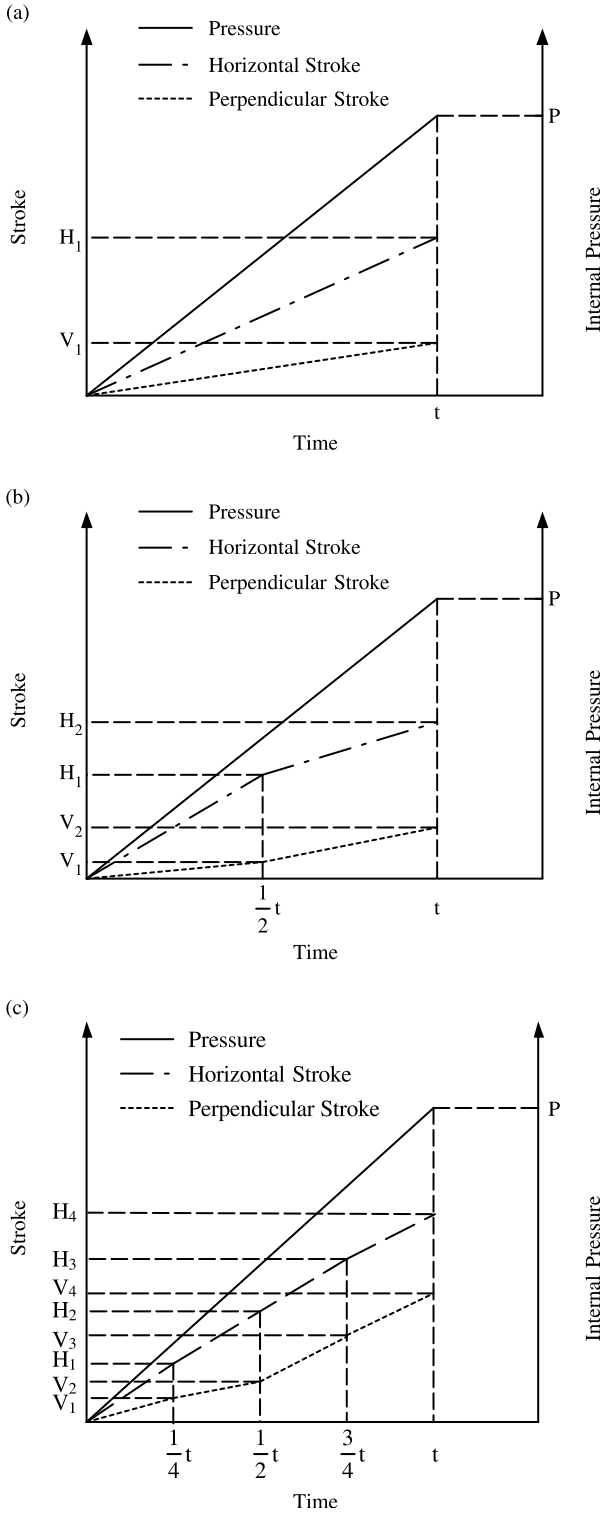

Fig. 8. Schematic of pressurizing path, horizontal and vertical strokes for (a) single-stroke, (b) double-stroke and (c) quadruple-stroke for T-joint die.

the change in the material flow direction. In all the performed simulations, maximum thinning occurs at the center of the T-branch top where the material is in contact with the vertical actuator. This figure also depicts that utilizing quadruple-stroke results in a slightly thinner T-branch top but higher thickening at the die entry.

Table 3
Optimized pressure and strokes for T-joint hydroforming die

	Single-stroke	Double-stroke	Quadruple-stroke
Pressure (MPa), P	45.74	45.92	47.63
Axial feed (mm), H	$H_1=5.58$	$H_1=2.17$	$H_1=4.14$
		$H_2=6.12$	$H_2=6.29$
			$H_3=6.76$
			$H_4=10.04$
Bulge control (mm), V	$V_1=6.24$	$V_1=3.31$	$V_1=4.75$
		$V_2=7.4$	$V_2=8.07$
			$V_3=8.7$
			$V_4=8.72$
T-branch height (mm)	6.05	7.17	8.29
Max. hoop strain (True)	0.228	0.258	0.277
Thickness deviation (Eq. 2)	8.75	10.34	9

2.2.2. Experimental results of t-joint tube hydroforming

To validate the above results, the optimized loading paths were employed to conduct T-joint experiments in the die shown in Fig. 7. Extruded aluminum tubes of 6063-T4 with the dimensions and lubrication conditions described for the closed-die experiments were used. After the tube was placed in the T-joint die cavity, axial actuators were brought into contact with tube-ends and the tube was then filled with mineral fluid. Perpendicular actuator was then advanced until it touched the tube surface. Single-, double-, and quadruple-stroke functions were assigned to the axial and vertical actuators, as determined from the above simulations. Fig. 10 shows the experimental results of T-joint hydroformed tubes. All the tubes were able to achieve

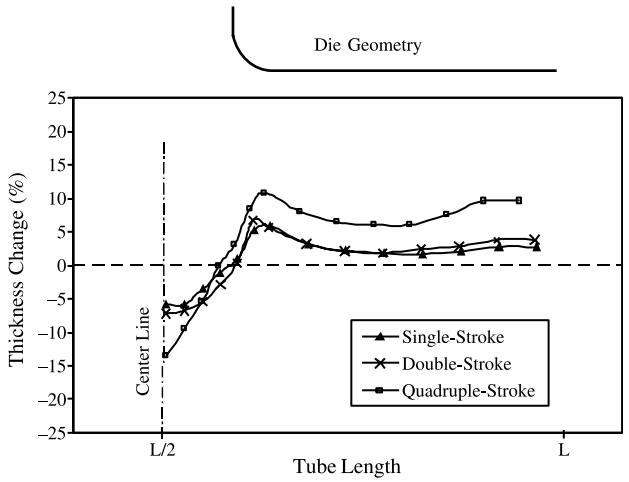

Fig. 9. Thickness distribution along the tube for various scenarios in T-joint tube hydroforming. For visualization convenience die geometry is also indicated.

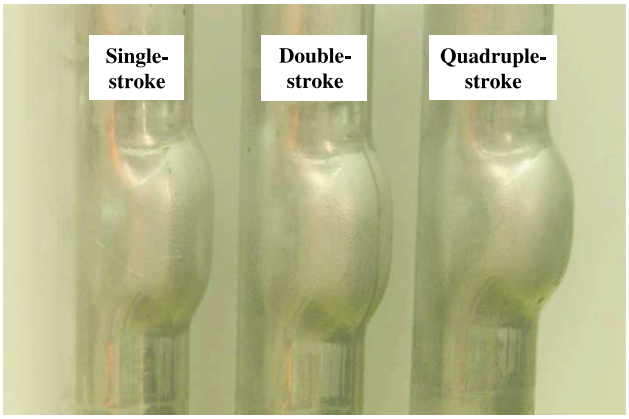

Fig. 10. Experimental results of T-joint hydroformed tubes utilizing optimized loading paths.

the predicted (Table 3) final T-branch height without experiencing any failure. In other words, quadruple-stroke loading path resulted in the highest bulge height followed by the double-, and the single-stroke functions. Since the axial feeds (H) and bulge control (V) obtained from simulations were assigned to the experiments, the T-branch height from the experiments was almost the same as those obtained from the simulations. Thus, the optimization method employed above was able to guide the experiments to achieve the desired result. It is also clear from the results that utilization of multiple strokes to form the T-joint yields better formability of the tube and consequently a higher bulge height.

The experimentally obtained T-branch shown in Fig. 10 may not be of sufficient height that can be of practical value. This is because of the low formability of the material used and also because of the specification of the constraint to limit the maximum stress induced in the material to be below the ultimate stress. In addition, it was aimed in the objective that the central 1/3rd portion of the T-branch top should reach the maximum bulge height. Because of these reasons the branch height obtained in the experiments was not significant. However, by choosing different constraints and objectives the attainable final branch height may be increased significantly. But the emphasis of the current article is to provide a methodology for optimization of process parameters. More in-depth results that focus on achieving industrially relevant geometries using different materials, heat treatments along with optimization of the process will be presented in future publications [16].

3. Discussion

In the above hydroforming experiments, providing sufficient amount of axial force to feed required material into the forming zone is a key issue. In other words, the material needs to be fed into the die cavity in a manner that ensures a uniform thickness distribution while keeping the induced stress lower than the ultimate stress. Internal pressure also plays a crucial role in tube deformation, material flow and conformance of the tube to the die geometry. The simulations and the optimization scheme on closed-die and T-joint suggest that to achieve an optimized final part, the majority of the end-feed should occur after the tube material yields. In other words, the tube should initially expand due to the internal pressure until plastic flow is initiated, and then further material needs to be supplied into the forming zone by means of axial feed. Thus, the material can flow more easily and a higher bulge can be achieved when small increments of stress can generate larger strains. However, at higher pressures, if sufficient axial feed is not provided, thinning is bound to occur which leads to failure as seen in closed-die hydroforming (Fig. 5(b)).

Nevertheless, if higher internal pressure is applied with suitable axial feed, failure can be avoided and a better conformance to the die shape may be achieved although this may not lead to an optimized thickness deviation. It is also evident that by utilizing quadruple-stroke, a slightly better conformance of the tube to the die shape or a higher bulge could be obtained. Although this may not have a significant role in the tube conformance for the current geometry, employing a larger number of strokes provides an opportunity to better meet the product design specifications, e.g. minimum thickness deviation, and achieve the desired final shape. FE simulations of the closed-die also showed that for all the cases considered, the maximum effective stress is induced at the die corner as the material curves to conform to the bent geometry. This could be due to the additional bending stress developed in the die corner.

Optimization of the T-joint hydroforming also predicts that employing multiple strokes to push the tube-ends results in a higher T-branch. The double-stroke and quadruple-stroke procedures show that the efficient way of making a T-joint is to allow the tube to bulge freely in the early stages of the process. Major axial feed needs to be provided subsequently to force the material into the forming region. It should be noted that in all simulations the maximum effective stress as well as maximum thinning occurred at the center of the T-branch. In addition, tube hydroforming experiments of the T-joint validated the results for all the cases considered. Using multiple strokes to feed the material and control the bulge height, a higher bulge height was successfully achieved as predicted by the simulations.

Utilizing optimized loading paths in tube hydroforming experiments are crucial for successful production of desired features in the final part. Although the current investigation focuses only on limited geometrical features and shapes, the optimization procedure discussed here can be effectively used under more complex scenarios with appropriate objectives and constraints. It is important to state that material formability limits should also be suitably

incorporated through appropriate failure criterion to obtain more realistic results and failure scenarios.

4. Conclusions

Based on the experiments and FE simulations performed the following conclusions are drawn:

- An optimization procedure was developed for tube hydroforming process with suitable objectives and constraints based on the desired geometrical features of closed-die and T-joint. Tube hydroforming experiments with the determined optimized loading paths were conducted and experimental results were found to be in good agreement with FE simulations.
- Employing higher internal pressure in the closed-die yields more severe thinning in the tube that causes tube burst. However, at the failure time, a higher bulge height was noticed for quadruple-stroke compared to double-stroke and single-stroke, respectively.
- Both closed-die and T-joint simulations revealed that to obtain the optimized thickness distribution (without failure), the majority of the end-feed should be applied after the tube material yields under internal pressure.
- Based on the obtained results for both closed-die and T-joint simulations and experiments, realistic formability of the tube material can be better realized when multiple-strokes are employed for axial and vertical actuators. FE simulations of the closed-die revealed that using multiple-strokes in the current scheme results in a slight enhancement of the tube conformance compared to the situation where single-stroke is used. Utilizing multi-stroke functions in the T-joint formation also resulted in an increase in the T-branch.

Acknowledgements

The authors sincerely acknowledge the support from Hydro Aluminum Technology Center NA, Holland, MI and Norwegian Research Council, Oslo, Norway.

References

[1] B. Budiansky, A reassessment of deformation theories of plasticity, ASME Journal of Applied Mechanics 26 (1959) 259–264.
[2] K.-i. Manabe, M. Amino, Effects of process and material properties on deformation process in tube hydroforming, Journal of Materials Processing Technology 123 (2002) 285–291.
[3] W. Rimkus, H. Bauer, M.J.A. Mihsein, Design of load-curves for hydroforming applications, Journal of Materials Processing Technology 108 (2000) 97–105.
[4] J.-B. Yang, B.-H. Jeon, S.-I. Oh, Design sensitivity analysis and optimization of the hydroforming process, Journal of Materials Processing Technology 113 (2001) 666–672.
[5] K.-J. Fann, P.-Y. Hsiao, Optimization of loading conditions for tube hydroforming, Journal of Materials Processing Technology 140 (2003) 520–524.
[6] Y. Aue-U-Lan, G. Ngaile, T. Altan, Optimizing tube hydroforming using process simulation and experimental verification, Journal of Materials Processing Technology 146 (2004) 137–143.
[7] S.-D. Liu, D. Meuleman, K. Thompson, Analytical and experimental examination of tubular hydroforming limits, Journal of Materials and Manufacturing 107 (1998) 287–297.
[8] N. Asnafi, A. Skogsgårdh, Theoretical and experimental analysis of stroke-controlled tube hydroforming, Journal of Materials Science and Engineering A (Switzerland) 279 (1/2) (2000) 95–110.
[9] M. Imaninejad, G. Subhash, A. Loukus, Experimental and numerical investigation of free-bulge formation during hydroforming of aluminum extrusions, Journal of Materials Processing Technology 147 (2004) 247–254.
[10] M. Imaninejad, G. Subhash, A. Loukus, Influence of end-conditions during tube hydroforming of aluminum extrusions, International Journal of Mechanical Sciences 46 (2004) 1195–1212.
[11] B.J. Mac Donald, M.S.J. Hashmi, Finite element simulation of bulge forming of a cross-joint from a tubular blank, Journal of Materials Processing Technology 103 (2000) 333–342.
[12] M. Ahmed, M.S.J. Hashmi, Three-dimensional finite-element simulation of bulge forming, Journal of Materials Processing Technology 119 (2001) 387–392.
[13] D.B. Marreco, H.A. Al-Qureshi, Forming of a Tee-Junction on metal tubes by an elastomer rod technique Seventh North American Metalworking Research Conference (1979), pp. 107–113.
[14] H.A. Al-Qureshi, L.A. Moriera Filho, Junction forming in aluminum tubes using an elastomer technique, Materials and Manufacturing Processes 16 (5) (2001) 717–724.
[15] L.A. Moriera Filho, H.A. Al-Qureshi, Elastomer forming of cross junction, International Journal of Machanical Tool Design Research 26 (4) (1986) 403–414.
[16] A. Loukus, G. Subhash, M. Imaninejad, Optimization of material properties and process parameters for tube hydroforming of aluminum extrusions, Journal of Engineering Materials and Technology, 2005, Submitted for Publication.